PHILOSOPHICAL TRANSACTIONS OF THE ROYAL SOCIETY A

CrossMark click for updates

Phil. Trans. R. Soc. A (2012) **370**, 5088–5100
doi:10.1098/rsta.2012.0019

Review

Storage ring measurements of the dissociative recombination of H_3^+

By Holger Kreckel[1,2,4,*], Annemieke Petrignani[1,†], Oldřich Novotný[1,5], Kyle Crabtree[2], Henrik Buhr[6,‡], Benjamin J. McCall[2,3] and Andreas Wolf[1]

[1]*Max Planck Institut für Kernphysik, Saupfercheckweg 1, 69117 Heidelberg, Germany*
[2]*Department of Chemistry, and* [3]*Department of Astronomy, University of Illinois at Urbana-Champaign, Urbana, IL 61801, USA*
[4]*Max Planck Institute für Astronomie, Königstuhl 17, 69117 Heidelberg, Germany*
[5]*Columbia Astrophysics Laboratory, Columbia University, 550 West 120th Street, New York, NY 10027, USA*
[6]*Faculty of Physics, Weizmann Institute of Science, Rehovot 76100, Israel*

The dissociative recombination (DR) of H_3^+ is a key process in interstellar chemistry. More than 30 experimental studies of the DR process have been published in the literature. The H_3^+ DR rate coefficient results obtained from these measurements, however, have not always been consistent. The outcome seems to depend on the experimental method, on the exact measurement procedure and sometimes even on the interpretation of the experimental data. In the past two decades, heavy-ion storage rings have become the working horse for DR measurements, as they provide a direct measurement of the DR products. Furthermore, storage ring measurements yield energy-resolved rate coefficients with unprecedented resolution that allow for detailed comparison with theory. DR results from different storage ring facilities have shown a remarkable consistency throughout the years and they provide additional information on break-up dynamics and internal excitation. In this study, we will review the storage ring DR measurements that have been carried out for H_3^+.

Keywords: electron recombination; dissociative recombination; storage ring

1. Introduction

The triatomic hydrogen ion (H_3^+) has long been recognized as one of the main reaction agents in interstellar clouds. In these cold and dilute environments, H_3^+

*Author for correspondence (holger.kreckel@mpi-hd.mpg.de).
†Present address: Leiden Observatory, Leiden University, 2300 RA Leiden, The Netherlands.
‡Present address: Physikalisch-Technische Bundesanstalt, Bundesallee 100, 38116 Braunschweig, Germany.

One contribution of 21 to a Theo Murphy Meeting Issue 'Chemistry, astronomy and physics of H_3^+'.

serves as a universal proton donor and thus enables the formation of larger molecules even at extremely low temperatures and densities. In the diffuse interstellar medium, the dissociative recombination (DR) with free electrons,

$$H_3^+ + e^- \rightarrow \begin{cases} H + H + H, \\ H_2 + H, \end{cases} \tag{1.1}$$

is the dominant destruction mechanism for H_3^+, and the DR rate coefficient at low temperature is one of the most crucial parameters of interstellar cloud models. Consequently, a lot of experimental and theoretical effort has been put into the determination of the H_3^+ DR rate in the past decades. For many years, the overall magnitude of the DR rate coefficient was the subject of controversy, as different experimental techniques disagreed by orders of magnitude. In particular, afterglow measurements yielded very low DR rate coefficients, in stark disagreement with storage rings. This discrepancy appears to have been cured very recently by a re-evaluation of the afterglow results—taking into account ternary collisions—that brings them into agreement with the storage ring experiments [1]. The history of H_3^+ DR measurements and the controversy surrounding the early measurements in afterglows has been summarized in previous reviews [2].

This study focuses on storage ring measurements, and it is organized as follows: in §2, we will briefly explain the storage ring technique. In §3, we review the DR rate coefficient results obtained for H_3^+. In §4, we will describe imaging techniques as temperature diagnostics for the excitation of stored molecular ions and present recent results for H_3^+. In §5, we will address the influence of nuclear spin. In §6, we will sum up the status and outline perspectives for future work.

2. Dissociative recombination in heavy-ion storage rings: the technique

The storage ring technique has been used for molecular recombination measurements since the early 1990s. Four different ion storage rings were used for DR measurements (in alphabetical order: ASTRID, Aarhus; CRYRING, Stockholm; TARN II, Tokyo; test storage ring (TSR), Heidelberg). Owing to the fundamental importance and the controversy surrounding the H_3^+ DR process, independent H_3^+ rate coefficient measurements were performed at all of these instruments. The basic concept was the same in all of the measurements. Figure 1 shows the Heidelberg TSR as an example. The H_3^+ ions are produced in an ion source and accelerated to mega-electronvolt energies, either inside the storage ring, or, in the case of the TSR, by external accelerators prior to ion injection. At these energies, the ions circulate a few hundred thousand times per second inside an ultra-high-vacuum beam pipe, where they are guided on a stable orbit by dipole and quadrupole magnets. Typical residual-gas-limited lifetimes of several seconds are achieved. All of the above-mentioned facilities were equipped with a mono-energetic electron beam device. In DR experiments, the electron beam has two functions: firstly, it is used to phase-space cool the molecular ions through Coulomb interactions; and secondly, the free electrons serve as a recombination target, inducing the DR process. For rate coefficient measurements, the neutral DR fragments are counted by semiconductor detectors at the end of a straight

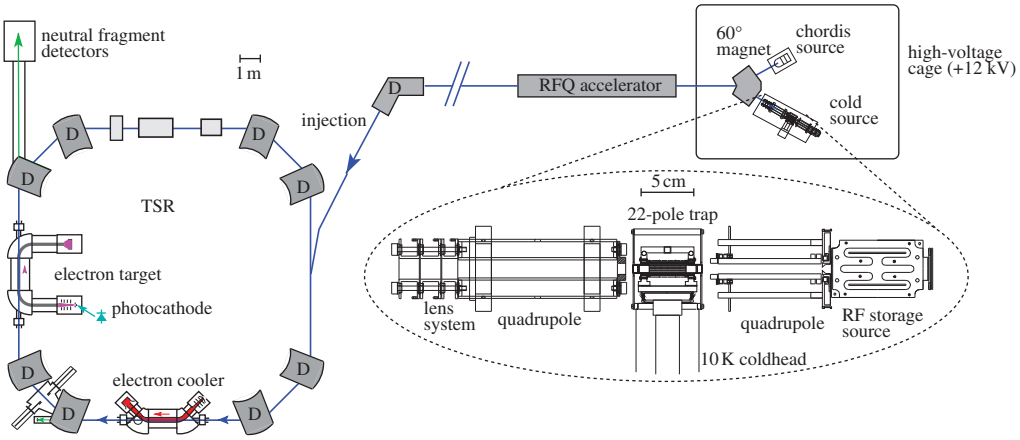

Figure 1. Overview of the test storage ring (TSR) facility of the Max Planck Institute für Kernphysik in Heidelberg, Germany. The molecular ions are produced in a dedicated ion source region and pre-accelerated to energies of several kilo-electronvolt per nucleon, before they are injected into a particle accelerator that brings them up to energies of several mega-electronvolt. Here, the linear radiofrequency quadrupole (RFQ) accelerator that is used for H_3^+ experiments is depicted. Also shown is the 22-pole ion trap setup that was developed as a cold ion injector for the TSR. The TSR features two cold electron beam setups, the electron target and the electron cooler, which can either be used independently, or in concert. The neutral recombination products are detected in the straight section downstream of the electron target. (Online version in colour.)

section downstream of the electron beam facility. In later experiments, detectors with imaging capabilities were used to analyse the break-up dynamics and for internal excitation diagnostics.

3. Dissociative recombination rate coefficient measurements of H_3^+

The H_3^+ ion was among the first molecular ions studied using the storage ring technique, with the initial measurement published by Larsson *et al.* [3]. A comparison of various storage ring rate coefficient measurements is shown in figure 2. The initial CRYRING experiment showed a smooth recombination rate as a function of the collision energy, the low-energy part of which could be modelled by a cross section $\sigma = 1.43 \times 10^{-16}/E^{1.15}\,\mathrm{cm}^2$ and resulted in a thermal rate coefficient of $1.15 \times 10^{-7}\,\mathrm{cm}^3\,\mathrm{s}^{-1}$ at 300 K [4]. In this measurement, the so-called direct DR peak at approximately 10 eV was observed for the first time. The experiment at CRYRING was followed by a measurement of the branching fraction between the two- and three-body channels that resulted in 75 per cent: $(H + H + H)$ and 25 per cent: $(H_2 + H)$ [5].

Subsequent rate coefficient measurements at both the TARN II storage ring [6] and at the ASTRID [7] were in fair agreement with the CRYRING results.

Shortly after the supporting experiments at ASTRID and TARN II, complementary imaging experiments at the TSR, aiming at the analysis of the internal excitation of stored H_3^+ ions ([8,9] and see also §4) revealed that conventional ion sources result in highly excited ions, corresponding to a rotational temperature of several thousand degrees Kelvin. Moreover, as H_3^+ has

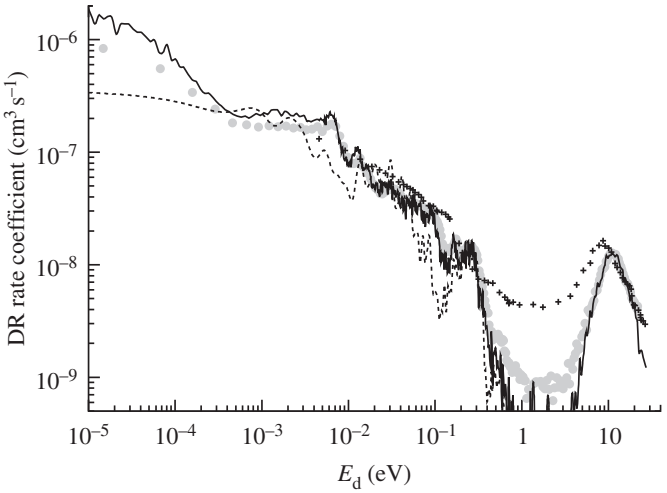

Figure 2. Comparison of various H_3^+ DR storage ring rate coefficients as a function of the detuning energy, E_d. The black pluses show the CRYRING measurements using an electron impact ion source (adapted from Le Padellec *et al.* [10]). The grey circles show the CRYRING measurement using a solenoid supersonic expansion source [11]. The black solid line depicts the 22-pole results from TSR, and the dashed line shows the theoretical calculation for a rotational temperature of 300 K (adapted from Petrignani *et al.* [12]). Note that the differences in the region between 0.4 and 10 eV stem from the influence of higher energetic electrons owing to the toroidal regions of the electron coolers. The more recent CRYRING and TSR data have been corrected for this effect, the initial *hot* CRYRING data are uncorrected.

no permanent dipole moment, it hosts metastable rotational states with lifetimes ranging from hours to several months [13]. These findings led to the development of *cold* ion sources, using active cooling of the rotational degrees of freedom. Two independent approaches were pursued.

The first approach used a supersonic expansion ion source driven by a solenoid valve. The ion source was calibrated by laser spectroscopy performed at the University of California, Berkeley and then shipped to CRYRING for the DR measurements. In the spectroscopy measurements, only the two lowest H_3^+ states were observed [14], and the DR rate coefficient recorded at CRYRING featured structures at low energy that had been absent in the previous data [11]. The thermal rate coefficient derived from this measurement is lower by approximately 40 per cent when compared with the previous CRYRING measurement obtained using a conventional ion source.

For the second approach, a cryogenic ion trap was developed as an injector for the TSR storage ring. In this 22-pole trap [15], the H_3^+ ions are confined by radiofrequency fields at a temperature of approximately 13 K. During storage inside the trap, the ions are actively cooled in collisions with the helium buffer gas. To perform spectroscopy inside the ion trap, a chemical-probing scheme was developed that showed that H_3^+ can indeed be cooled down to its lowest rotational states inside the trap [16]. The DR measurements carried out with the 22-pole injector [17] are in very good agreement with the *cold* CRYRING results. Owing to the comparatively low number of ions, the DR measurements using the 22-pole injector could not be calibrated on an absolute scale; therefore,

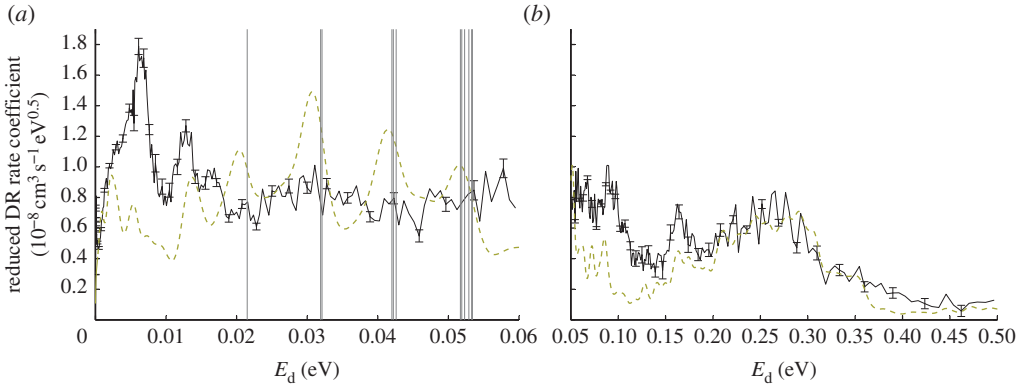

Figure 3. Reduced DR rate coefficient versus detuning energy. The measurement (solid line) was carried out at TSR using the 22-pole ion source. The calculation (dashed line) represents a rotational temperature of 300 K. (*a*) The energy range from 0 to 0.06 eV is shown, vertical lines mark excited rotational thresholds that could lead to the opening of a Rydberg series of resonances. (*b*) The energy range from 0.05 to 0.5 eV is shown. Adapted from Petrignani *et al.* [12]. (Online version in colour.)

they were normalized to the CRYRING results at the high-energy peak around 10 eV. Despite the common absolute calibration, it is remarkable that these two experiments which were carried out at different facilities with different ion sources, different beam energies and measurement schemes are in very good agreement with one another over the entire energy range. In a recent TSR experiment, additional rate coefficient data were taken, using a piezo-driven version of the supersonic expansion ion source, and an independent absolute calibration was performed, based on the beam lifetime difference with and without electrons present. This measurement confirms once more both the previous CRYRING measurement and the 22-pole data across the entire energy range [18]. Further support comes from modern theoretical calculations of the H_3^+ DR process that identify the mechanism driving the DR process at low energies and agree with the storage ring results on the magnitude of the process [19–21]. A simplified analytical treatment of the H_3^+ DR recombination process by Jungen & Pratt [22] also finds good agreement with the overall scale of the measured DR rate coefficient.

In the light of these developments, the H_3^+ DR problem appeared essentially solved [23]. However, the origin of the resonant structures that are observed at low energies is still uncertain. Dos Santos *et al.* [21] performed rate coefficient calculations at various rotational temperatures, coming to the conclusion that the actual rotational temperature of the ions inside the storage rings is probably higher than assumed. Very recent imaging experiments that support this conclusion will be presented in §4*b*.

Figure 3 shows a comparison of TSR storage ring measurements with state-of-the-art theoretical calculations, assuming a rotational temperature of 300 K. To allow for a detailed comparison, the data are shown on linear scales. Furthermore, the reduced rate coefficient $\langle\alpha\rangle\sqrt{E_d}$ is plotted to eliminate the inherent $1/\sqrt{E_d}$ dependence at low energies. The measured structures at very low energy (0–0.06 eV) are not well represented by theory, and the calculated rotational

thresholds do not coincide with structures in the experimental data. It is presently unclear whether these remaining discrepancies are due to experimental problems at low energy, or whether theory needs further refinement. In the higher energy range from 0.05 to 0.5 eV, the picture is more encouraging, with fair agreement between 0.2 and 0.5 eV. More information on the calculations can be found in the original publication [12].

4. Vibrational and rotational diagnostics

(*a*) *Monitoring vibrational excitations of* H_3^+ *by Coulomb explosion imaging*

The initial vibrational level of a molecular ion can have a major impact on the DR rate coefficient. In fact, the traditional DR concept after Bates requires a curve crossing between the initial ionic state and a dissociative neutral state into which the electron is captured. For H_3^+, no such curve crossing exists at low energies, and thus theoretical calculations in the 1980s [24] predicted that the DR cross section is negligibly small for $H_3^+(v=0)$ and becomes significant only for $H_3^+(v \geq 3)$. Supported by afterglow experiments [25], this notion was perpetuated well into the 1990s [26].

In storage ring experiments, vibrational cooling is usually achieved by storing the ions for a few seconds before commencing the DR measurement. For most molecules that time span is sufficient for complete vibrational relaxation by spontaneous emission of photons. In the case of H_3^+, however, there were doubts concerning the time scale of vibrational cooling because one of the normal modes—namely the symmetric stretch mode—is infrared inactive and thus has unusually long lifetimes. To monitor the vibrational decay during the first seconds of storage, Coulomb explosion imaging (CEI) measurements were performed at the TSR. In this experiment, a small fraction of the stored H_3^+ ions are peeled off by a slow extraction technique and guided into a dedicated CEI beamline, where the ions are directed towards a thin target foil (thickness less than 100 Å). Inside the foil, the binding electrons are stripped off within the first 100 attoseconds, whereas the protons traverse the foil (see figure 4*a* for a sketch of the CEI principle). The electron stripping is much faster than the nuclear motion inside the molecule; therefore, the proton positions can be considered frozen during the stripping process. Behind the target foil, the protons repel each other strongly owing to the Coulomb force and, after a flight distance of several metres, they have gained distances of a few centimetres. The spatial distances and the different impact times are recorded by a three-dimensional imaging detector. While the relative proton distances are recorded for single molecular events at a time, for an ensemble of events, the measured distribution reflects the quantum mechanical probability density as given by the square of the nuclear wave function. As vibrational excitation modifies the nuclear wave function, the CEI method allows for direct monitoring of the vibrational decay of the H_3^+ ions inside the storage ring.

In figure 4*b*, the outcomes of the H_3^+ CEI measurements are shown. Here, we focus only on the symmetric stretch coordinate v_a, as those vibrational states have the longest lifetimes. For very short storage times of less than 1 ms, a broad distribution was observed that narrows down significantly during the first 2 s of storage and then remains stable. The data taken after 2 s are in very

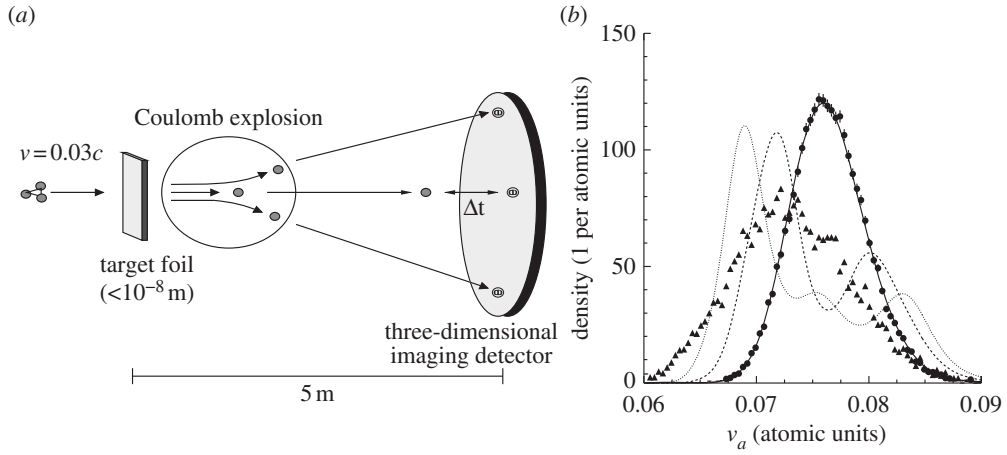

Figure 4. (*a*) Sketch of the Coulomb explosion imaging (CEI) principle. See text for details. (*b*) CEI results for H_3^+. Plotted is the sum of the relative velocities of the three protons $v_a = (v_{12} + v_{23} + v_{31})/\sqrt{3}$. The v_a coordinate is directly related to the initial size of the molecule, which reflects the symmetric stretch normal mode. The triangles depict the CEI results for storage times < 1 ms, the circles show the CEI results for times > 2 s. The solid curve shows a Monte Carlo simulation of the Coulomb explosion process based on the vibrational ground state. The dashed and dotted lines show the first $(1,0^0)$ and second $(2,0^0)$ excited states of the symmetric stretch mode, respectively.

good agreement with a simulation of the Coulomb explosion process assuming all the molecules to be in their ground vibrational state, clearly demonstrating that 2 s of storage are indeed sufficient for complete vibrational relaxation. However, the data taken at shorter storage times revealed an interesting twist. In a more detailed analysis [9], it was possible to fit the wave functions of the vibrationally excited states $(1,0^0)$ and $(2,0^0)$ to the data and watch the contribution of those symmetric stretch states decay spontaneously inside the ring. The lifetimes observed in this fashion were much shorter than the theoretical predictions for those vibrational bands [27]. In order to explain this behaviour, a comprehensive ro–vibrational relaxation model was created that was able to reproduce the extended lifetimes [13]. Strong indications were found that highly excited rotational states with an estimated effective temperature of approximately 3000 K are responsible for speeding up the vibrational decay through couplings between the rotational and vibrational motion. These findings were corroborated by DR fragment imaging results that found evidence for the presence of highly excited rotational states, even after 60 s of storage [8]. Indeed, many of the long-lived rotational states in H_3^+ are quasi-stable and can have lifetimes of several months [13].

The combination of the earlier-mentioned experiments and models identified the rotational excitation as the main obstacle for storage ring DR measurements with cold H_3^+, while vibrational excitation was found to be mostly harmless.

(*b*) *Rotational excitation by dissociative recombination fragment imaging*

For DR fragment imaging experiments, the surface barrier detector, which is used for rate coefficient measurements in the straight detection section

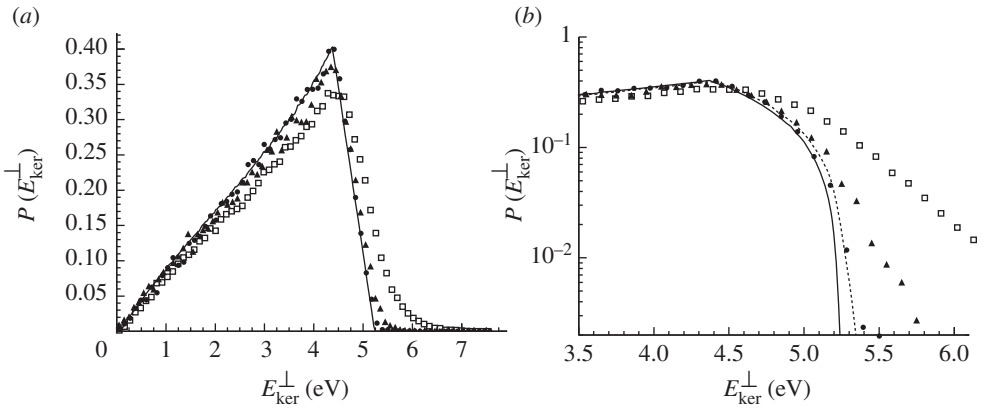

Figure 5. Transverse kinetic energy release distributions of the three-body breakup of H_3^+. All measurements were taken at the TSR, using the electron target. The second electron beam device—the electron cooler—can be switched on or off to provide additional cooling. The open squares depict measurements with a hot Penning ion source. The triangles show measurements with the Piezo expansion source and the solid dots show measurements taken with the 22-pole ion trap (in both cases, the electron cooler was off). The solid line shows a simulated distribution for 0 K rotational temperature. (*a*) The entire distribution is plotted. (*b*) A logarithmic plot of the high-energy region with the addition of a dashed line that depicts a 400 K simulation. For the data plotted here, para-H_2 was used as a precursor gas for both the supersonic expansion source and for the 22-pole injector; however, data taken with normal-H_2 showed no statistically significant difference in the imaging results.

downstream of the electron beam, is replaced by a position-sensitive detector. The fragment distances are recorded for a single molecular event at a time. Here, we focus on the three-body breakup

$$H_3^+ \longrightarrow H(1s) + H(1s) + H(1s). \tag{4.1}$$

In the two-body channel, the internal excitation of the outgoing H_2 fragment introduces an additional uncertainty and makes this pathway less informative for the diagnostic of the initial molecular excitation. For the three-body breakup, all three H atoms are in the electronic ground state and thus—together with the well-known relative electron–ion collision energy—the recorded distance distribution can be directly related to the initial excitation of the molecule. Most DR imaging experiments use a two-dimensional detector that records the transverse particle distances but not the relative impact times. The shape of the expected two-dimensional distance distribution can be predicted and simulated very reliably, assuming a random orientation of the molecules in the ring and taking into account the finite electron–ion overlap length in the electron target/cooler.

The sum of the transverse interparticle distances $R^2 = R_{12}^2 + R_{23}^2 + R_{31}^2$ translates directly into the *transverse* kinetic energy release by

$$E_{ker}^{\perp} = \frac{1}{3s^2} E_{beam} R^2, \tag{4.2}$$

where s is the average flight distance to the detector (measured from the centre of the electron target) and E_{beam} stands for the ion beam energy. For ground state H_3^+ and $E_{\mathrm{d}} = 0\,\mathrm{eV}$, one expects a kinetic energy release of 4.790 eV [12].

Figure 5*a* shows a comparison of imaging results from the TSR for different ion sources and conditions. The TSR is equipped with two independent cold electron beam devices. For all imaging measurements, the electron target is used, whereas the electron cooler can be switched on or off to provide additional cooling. Also shown is a simulation for cold H_3^+ ions. Figure 5*b* shows a logarithmic representation of the high kinetic energy region. It is important to note that the statistically significant portion of the energy release spectrum lies not in the extreme tails of the distribution, but rather at $E_{\mathrm{ker}}^{\perp} < 5.2\,\mathrm{eV}$. By fitting simulations with various degrees of rotational excitation to the data and optimizing the χ^2, we were able to assign effective temperatures to the different datasets. The piezo source with the electron cooler off resulted in a temperature of $950 \pm 100\,\mathrm{K}$; however, by continuous cooling with both electron beams, the effective temperature could be lowered to $450 \pm 100\,\mathrm{K}$. The reason for the significantly higher temperature, when compared with spectroscopic measurements in the expansion region, is not fully understood. At present, it is believed that the ions were heated by the acceleration out of the ion source and that the same heating effect also applies to all previous expansion source measurements.

For the 22-pole trap data that were obtained without the strong additional electron cooler beam, the χ^2 values for fits of simulated distributions with temperatures more than 300 K were identical within the uncertainties. However, the only rate coefficient measurement obtained using the 22-pole trap, with imaging measurements performed under the same conditions, was carried out using both the electron cooler beam and the electron target beam at the same time. In this case, the temperature inferred from the imaging results is $380^{+50}_{-130}\,\mathrm{K}$ (for details, see Petrignani *et al.* [12]). This measurement is the coldest storage ring measurement of the DR of H_3^+ with independent temperature evaluation on record.

5. The influence of nuclear spin

Similar to molecular hydrogen, H_3^+ exists in two different nuclear spin modifications. The three proton spins can either combine to a nuclear spin of $I = 3/2$, corresponding to ortho-H_3^+, or to $I = 1/2$, corresponding to para-H_3^+. Spontaneous conversion between these two nuclear spin states is extremely slow. The lowest rotational state of H_3^+ ($J = 1, G = 1$), is of para symmetry, whereas the next state ($J = 1, G = 0$), which lies approximately 30 K higher in energy, is of ortho symmetry. In astrophysical observations, typically, lines from both states are observed.

In the high-temperature limit, the ortho/para fraction in H_3^+ is 1 : 1. By sympathetically cooling H_3^+ ions to temperatures less than 50 K, e.g. in collisions with helium buffer gas, this fraction will be maintained and result in equal populations in the two lowest rotational states. In order to measure nuclear-spin-selective DR rate coefficients, it is necessary to manipulate the ortho/para fraction in a controlled fashion in the ion source. The first attempt was made at the TSR using the 22-pole injector [17]. In this experiment, para-H_2 was used

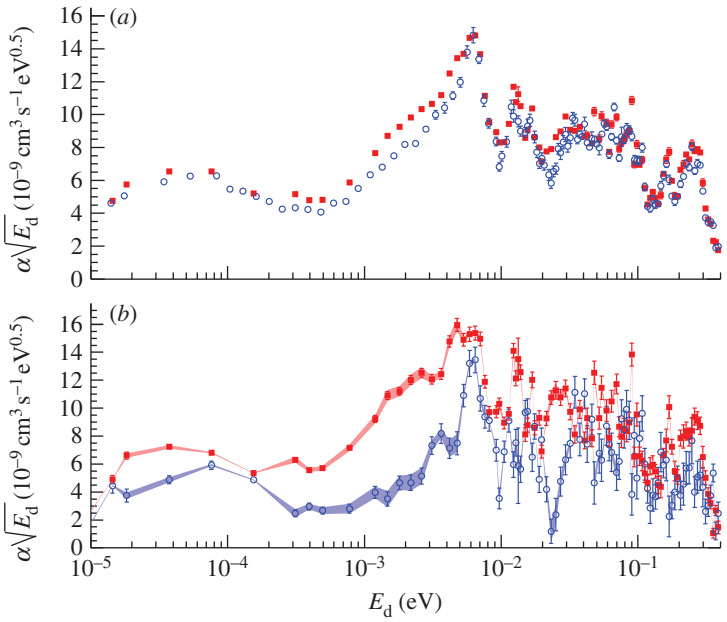

Figure 6. Reduced DR rate coefficient of H_3^+ measured using a supersonic expansion source. (*a*) Results using gas mixtures of 1 : 5 normal-H_2 : Ar (circles) and 1 : 5 para-H_2 : Ar (squares). (*b*) Extrapolated results for 100% para-H_3^+ (squares) and 100% ortho-H_3^+ (circles) are shown. For the extrapolation, a para-H_3^+ fraction of (47.9 ± 2)% for normal-H_2 : Ar and (70.8 ± 2)% for para-H_2 : Ar in the initial measurement is assumed, as obtained by cavity ring-down spectroscopy in the expansion region (see discussion in the text). Adapted from Kreckel *et al.* [18]. (Online version in colour.)

as a precursor gas in the ion source, and a slight enhancement of the DR rate coefficient at low energies was observed. Unfortunately, it was not possible to determine the enrichment in the para-H_3^+ fraction that was achieved. To improve on this first experiment, a second measurement was carried out using a piezo-driven supersonic expansion ion source. The ortho/para ratio in H_3^+ was measured at the University of Illinois by cavity ring-down spectroscopy. Again, para-H_2 was used as a precursor gas to enrich the para-H_3^+ fraction. Owing to restrictions of the para-H_2 generator at the TSR, the hydrogen gas had to be diluted with argon in a mixture H_2 : Ar of 1 : 5 to achieve pressures that were sufficient for the expansion source. The same mixtures were used for the spectroscopy measurements. It was found that while the use of normal-H_2 yielded a para-H_3^+ fraction of (48 ± 2)%, consistent with the expected high-temperature value, the use of para-H_2 in the ion source resulted in a para-H_3^+ fraction of (71 ± 2)%. Furthermore, from the intensity ratio of the two lowest para-H_3^+ states, a rotational temperature of 180 K was inferred.

In figure 6, the low-energy DR rate coefficient is shown for the normal-H_2 : Ar and para-H_2 : Ar mixtures. At higher energies, both datasets merge and are identical within the error bars. The rate coefficient has been multiplied by $\sqrt{E_d}$ in all cases to eliminate the inherent $1/v$ dependence. As in previous measurements,

an enhancement of the rate coefficient is seen for the para-enriched data. In figure 6*b*, an extrapolation to 'pure' para-H_3^+ and 'pure' ortho-H_3^+ is shown. It should be kept in mind, though, that the temperature difference between the spectroscopic measurements (approx. 180 K) and the DR imaging results without using the strong electron beam of the electron cooler (approx. 950 K) implies that there is a heating process between ion production and the DR events. Most likely, the rotational excitation is induced by collisions with H_2 in the acceleration section downstream of the expansion region. Through proton exchange, these collisions might also alter the nuclear spin of H_3^+. Nevertheless, figure 6*b* shows, for the first time, detailed differences in the rate coefficient for para- and ortho-H_3^+ at low energies. Further experiments with the expansion source and an optimized acceleration scheme to avoid unwanted heating are foreseen.

6. Conclusion and perspectives

Already now the DR of H_3^+ deserves a special place in the history of electron recombination measurements. No other molecular ion has been examined as frequently and as thoroughly as H_3^+. The authors alone have been involved in H_3^+ DR measurements at the TSR using six different ion sources. Comparable efforts were made at CRYRING. The continuing efforts at the afterglow setups at Charles University in Prague have finally led to a better understanding of the recombination in hydrogen plasmas. Today, with perfect harmony among the storage ring measurements, with good agreement between theory and experiment on the absolute scale of the process and with the discrepancy to the afterglow experiments reconciled, it seems that at least the absolute value of the DR rate coefficient at low energies is well established.

An open question is still the difference in the rate coefficient of the lowest ortho- and para-H_3^+ states, as theory predicts a much larger effect than observed in the TSR measurement [21]. Recent absorption measurements in He–Ar–H_2 plasmas at 77 K seem to support theory [28]. Renewed significance for a precise determination of the individual rate coefficients of the lowest rotational H_3^+ states comes from observation in the diffuse interstellar medium that reveal an enigmatic difference in the ortho/para excitation temperatures of H_3^+ and H_2 [29].

The ideal DR experiment would comprise preparation of H_3^+ ions in a single ro–vibrational state and spectroscopic analysis, to yield state-selective rate coefficients. The new Cryogenic Storage Ring at the Max Planck Institut für Kernphysik (Heidelberg) combined with the 22-pole ion trap injector will be a great stride towards these optimal conditions.

References

1 Glosík, J., Plašil, R., Korolov, I., Kotrík, T., Novotný, O., Hlavenka, P., Dohnal, P. & Varju, J. 2009 Temperature dependence of binary and ternary recombination of H_3^+ ions with electrons. *Phys. Rev. A* **79**, 052707. (doi:10.1103/PhysRevA.79.052707)

2 Larsson, M. 2000 Experimental studies of the dissociative recombination of H_3^+. *Phil. Trans. R. Soc. Lond. A* **358**, 2433–2444. (doi:10.1098/rsta.2000.0658)

3 Larsson, M. *et al.* 1993 Direct high-energy neutral-channel dissociative recombination of cold H_3^+ in an ion storage ring. *Phys. Rev. Lett.* **70**, 430–433. (doi:10.1103/PhysRevLett.70.430)

4 Sundström, G. *et al.* 1994 Destruction rate of H_3^+ by low-energy electrons measured in a storage-ring experiment. *Science* **263**, 785–787. (doi:10.1126/science.263.5148.785)

5 Datz, S., Sundström, G., Biedermann, C., Broström, L., Danared, H., Mannervik, S., Mowat, J. R. & Larsson, M. 1995 Branching processes in the dissociative recombination of H_3^+. *Phys. Rev. Lett.* **74**, 4099. (doi:10.1103/PhysRevLett.74.4099.2)

6 Tanabe, T. *et al.* 2000 Dissociative recombination at the TARN II storage ring. In *Dissociative recombination: theory, experiment and applications*, vol. IV (eds M. Larsson, J. B. A. Mitchell & I. F. Schneider), pp. 170–179. Singapore: World Scientific.

7 Jensen, M. J., Pedersen, H. B., Safvan, C. P., Seiersen, K., Urbain, X. & Andersen, L. H. 2001 Dissociative recombination and excitation of H_3^+. *Phys. Rev. A* **63**, 052701. (doi:10.1103/3PhysRevA.63.052701)

8 Strasser, D. *et al.* 2001 Two- and three-body kinematical correlation in the dissociative recombination of H_3^+. *Phys. Rev. Lett.* **86**, 779–782. (doi:10.1103/PhysRevLett.86.779)

9 Kreckel, H. *et al.* 2002 Vibrational and rotational cooling of H_3^+. *Phys. Rev. A* **66**, 052509. (doi:10.1103/PhysRevA.66.052509)

10 Le Padellec, A., Larsson, M., Danared, H., Larson, A. A., Peterson, J. R., Rosén, S., Semaniak, J. & Strömholm, C. 1998 A storage ring study of dissociative excitation and recombination of D_3^+. *Phys. Scr.* **57**, 215–221. (doi:10.1088/0031-8949/57/2/010)

11 McCall, B. J. *et al.* 2003 An enhanced cosmic-ray flux towards ζ Persei inferred from a laboratory study of the H_3^+–e^- recombination rate. *Nature* **422**, 500–502. (doi:10.1038/nature01498)

12 Petrignani, A. *et al.* 2011 Resonant structure of low-energy H_3^+ dissociative recombination. *Phys. Rev. A* **83**, 032711. (doi:10.1103/PhysRevA.83.032711)

13 Kreckel, H., Tennyson, J., Schwalm D., Zajfman, D. & Wolf, A. 2004 Rovibrational relaxation model for H_3^+. *New J. Phys.* **6** 151. (doi:10.1088/1367-2630/6/1/151)

14 McCall, B. J. Huneycutt, A. J. & Saykally, R. J. 2004 Dissociative recombination of rotationally cold H_3^+. *Phys. Rev. A* **70**, 052716. (doi:10.1103/PhysRevA.70.052716)

15 Gerlich, D. 1995 Ion-neutral collisions in a 22-pole trap at very low energies. *Phys. Scr.* **59**, 256–263. (doi:10.1088/0031-8949/1995/T59/035)

16 Kreckel, H. *et al.* 2007 Electron collisions and rovibrational action spectroscopy of cold H_3^+ molecules. *J. Phys. Conf. Ser.* **88**, 012064. (doi:10.1088/1742-6596/88/1/012064)

17 Kreckel, H. *et al.* 2005 High-resolution dissociative recombination of cold H_3^+ and first evidence for nuclear spin effects. *Phys. Rev. Lett.* **96**, 263201. (doi:10.1103/PhysRevLett.95.263201)

18 Kreckel, H. *et al.* 2010 High-resolution storage-ring measurements of the dissociative recombination of H_3^+ using a supersonic expansion ion source. *Phys. Rev. A* **82**, 042715. (doi:10.1103/PhysRevA.82.042715)

19 Kokoouline, V., Greene, C. H. & Esry, B. D. 2001 Mechanism for the destruction of H_3^+ ions by electron impact. *Nature* **412**, 891–894. (doi:10.1038/35091025)

20 Kokoouline, V. & Greene, C. H. 2003 Unified theoretical treatment of dissociative recombination of D_{3h} triatomic ions: application to H_3^+ and D_3^+. *Phys. Rev. A* **68**, 012703. (doi:10.1103/PhysRevA.68.012703)

21 Dos Santos, S. F., Kokoouline, V. & Greene, C. H. 2007 Dissociative recombination of H_3^+ in the ground and excited vibrational states. *J. Chem. Phys.* **127**, 124309. (doi:10.1063/1.2784275)

22 Jungen, C., Pratt, S. T. 2009 Jahn–Teller interactions in the dissociative recombination of H_3^+. *Phys. Rev. Lett* **102**, 023201. (doi:10.1103/PhysRevLett.102.023201)

23 Larsson, M., McCall, B. J. & Orel, A. E. 2008 The dissociative recombination of H_3^+: a saga coming to an end? *Chem. Phys. Lett.* **462**, 145–151. (doi:10.1016/j.cplett.2008.06.069)

24 Michels, H. H. & Hobbs, R. H. 1984 Low-temperature dissociative recombination of $e + H_3^+$. *Astrophys. J. Lett.* **286,** L27–L29. (doi:10.1086/184378)

25 Adams, N. G., Smith, D. & Alge, E. 1984 Measurements of dissociative recombination coefficients of H_3^+, HCO^+, N_2H^+, and CH_5^+ at 95 and 300 K using the FALP apparatus. *J. Chem. Phys.* **81**, 1778–1784. (doi:10.1063/1.447849)

26 Smith, D. & Spanel, P. 1993 Dissociative recombination of H_3^+ and some other interstellar ions: a controversy resolved. *Int. J. Mass Spectrom. Ion Proc.* **129**, 163–182. (doi:10.1016/0168-1176(93)87040-Y)

27 Dinelli, B. M., Miller, S. & Tennyson, J. 1992 Bands of H_3^+ up to $4\nu_2$: rovibrational transitions from first principles calculations. *J. Mol. Spectrosc.* **153**, 718–725. (doi:10.1016/0022-2852(92)90506-J)

28 Varju, J., Hejduk, M., Dohnal, P., Jílek, M., Kotrík, T., Plašil, R., Gerlich, D. & Glosík J. 2011 Nuclear spin effect on recombination of H_3^+ ions with electrons at 77 K. *Phys. Rev. Lett.* **106**, 203201. (doi:10.1103/PhysRevLett.106.203201)

29 Crabtree, K. N., Indriolo, N., Kreckel, H., Tom, B. A. & McCall, B. J. 2011 On the ortho:para ratio of H_3^+ in diffuse molecular clouds. *Astrophys. J.* **729**, 15. (doi:10.1088/0004-637X/729/1/15)